

1 Introduction

Two sources of ULF waves in the ionosphere:

- Internal sources related to processes in the disturbed ionosphere, such as plasma irregularities
- External sources from active processes in regions above and below the ionosphere.

Those from above come mainly from the magnetosphere, and are referred to as **magnetospheric ULF waves** in this study. Those from below could be the result of lightning occurring in the atmosphere.

Waves excited by either internal sources or external sources in the lower atmosphere are referred to as **non-magnetospheric ULF waves**.

The majority of previous studies

have recognized that ULF waves in the magnetosphere can propagate into the ionosphere either as the fast mode, the Alfvén mode, or a combination of both.

Some recent studies

suggest that ULF magnetic fluctuations in the ionosphere may not be of magnetospheric origin.

The objective of this study is to investigate the characteristics of ULF waves from different sources, as observed in the ionosphere.

2 ULF wave detection

2.1 DEMETER satellite and its electric field data in the DC/ULF range

The DEMETER satellite was launched into a polar, nearly circular orbit on June 29, 2004.

- Altitude: 710 km at the early stage, lowered to 660 km since December 2005.
- Two local times: 10:30 LT (dayside) and 22:30 LT (nightside).

The electric field data in the DC/ULF range

- Sampling frequency of 39.0625 Hz
- A resolution of $\sim 40\mu\text{V/m}$
- Radial (E_r), azimuthal (E_{ϕ}) and parallel (E_{\parallel}) components
- May 2005 to November 2010, ~ 5.5 years

2.2 Main types of ULF waves on the nightside observed by the DEMETER satellite

ULF oscillations by DEMETER mostly occur on the nightside (Ouyang et al., 2018). According to latitudes where these nightside ULF oscillations occur, we may categorize them into **three main types**.

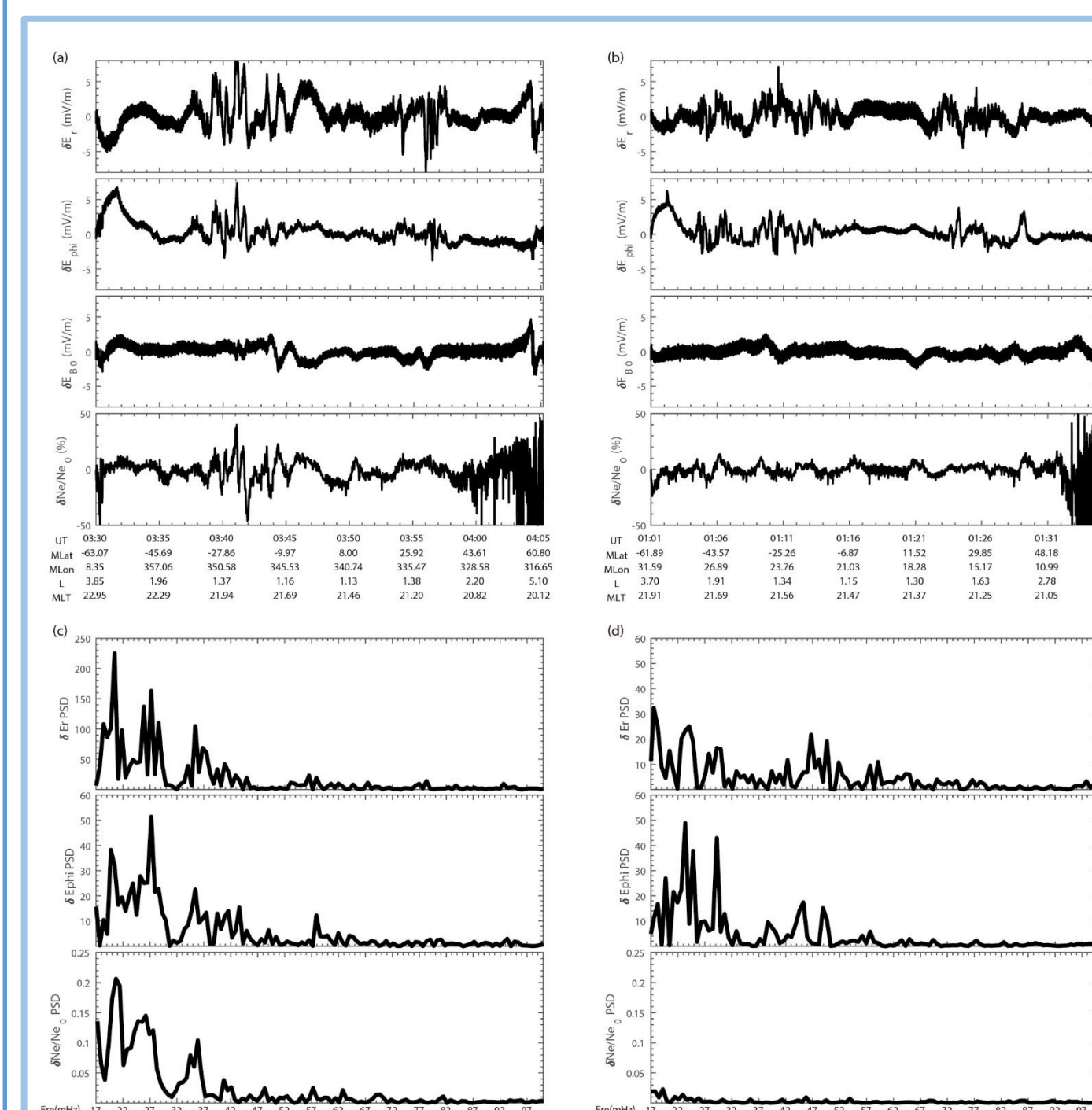
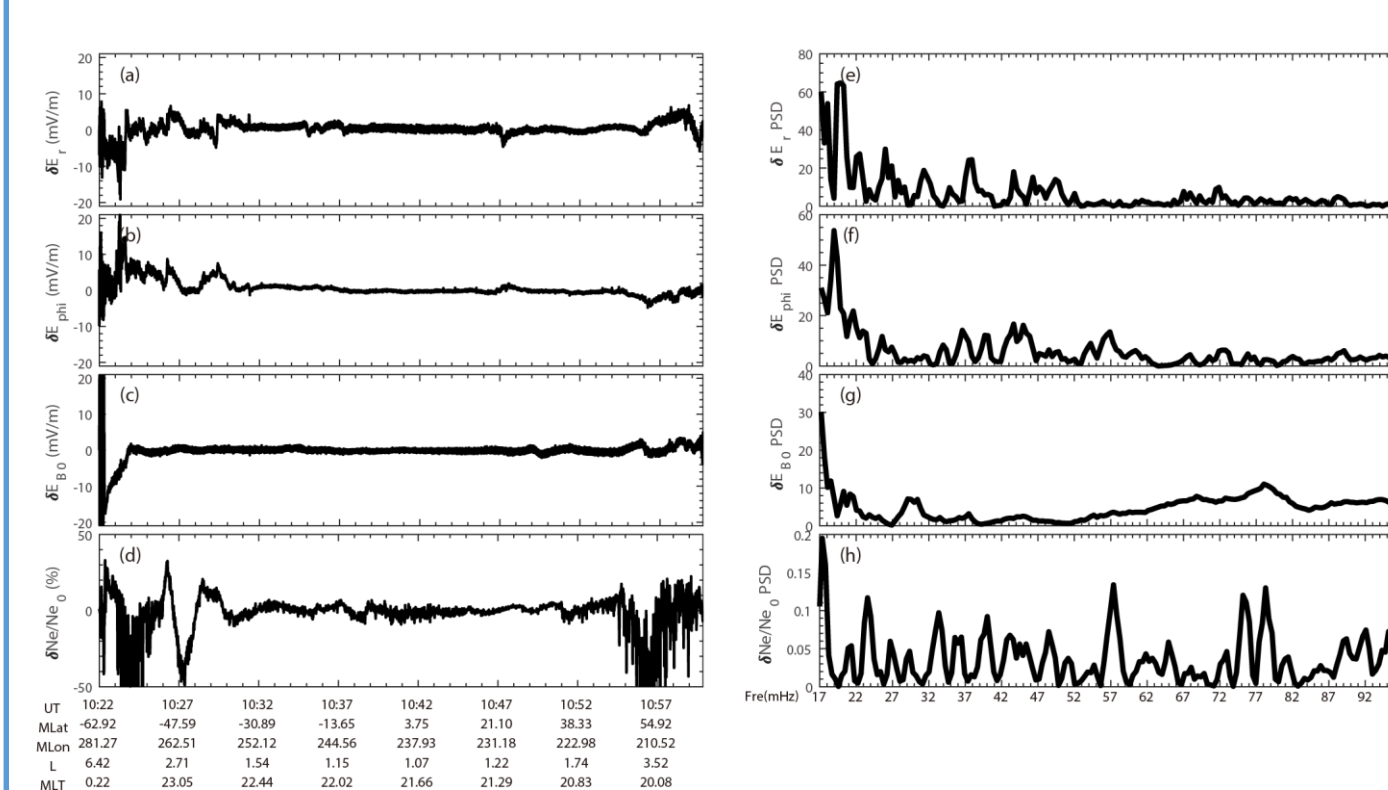


Figure 1. Examples of type I & type II

- Type I, ULF oscillations of the detrended electric field waveforms with simultaneous Ne perturbations
- Type II, without simultaneously significant Ne perturbations
- The power spectral density (PSD) in $L<2$ region for the type I event
- PSD in $L<2$ region for the type II event

Ouyang et al. (2018)



- To simplify, we categorize ULF oscillations at higher latitudes, in other words, not classified into type I and II, as type III
- Figure 2. Example of type III**
- Type III ULF oscillations at higher latitudes
 - Type III ULF oscillations at higher latitudes
 - PSD in $L>2$ region corresponding to (a-d)
 - PSD in $L>2$ region corresponding to (a-d)

2.3 ULF wave detection methodology

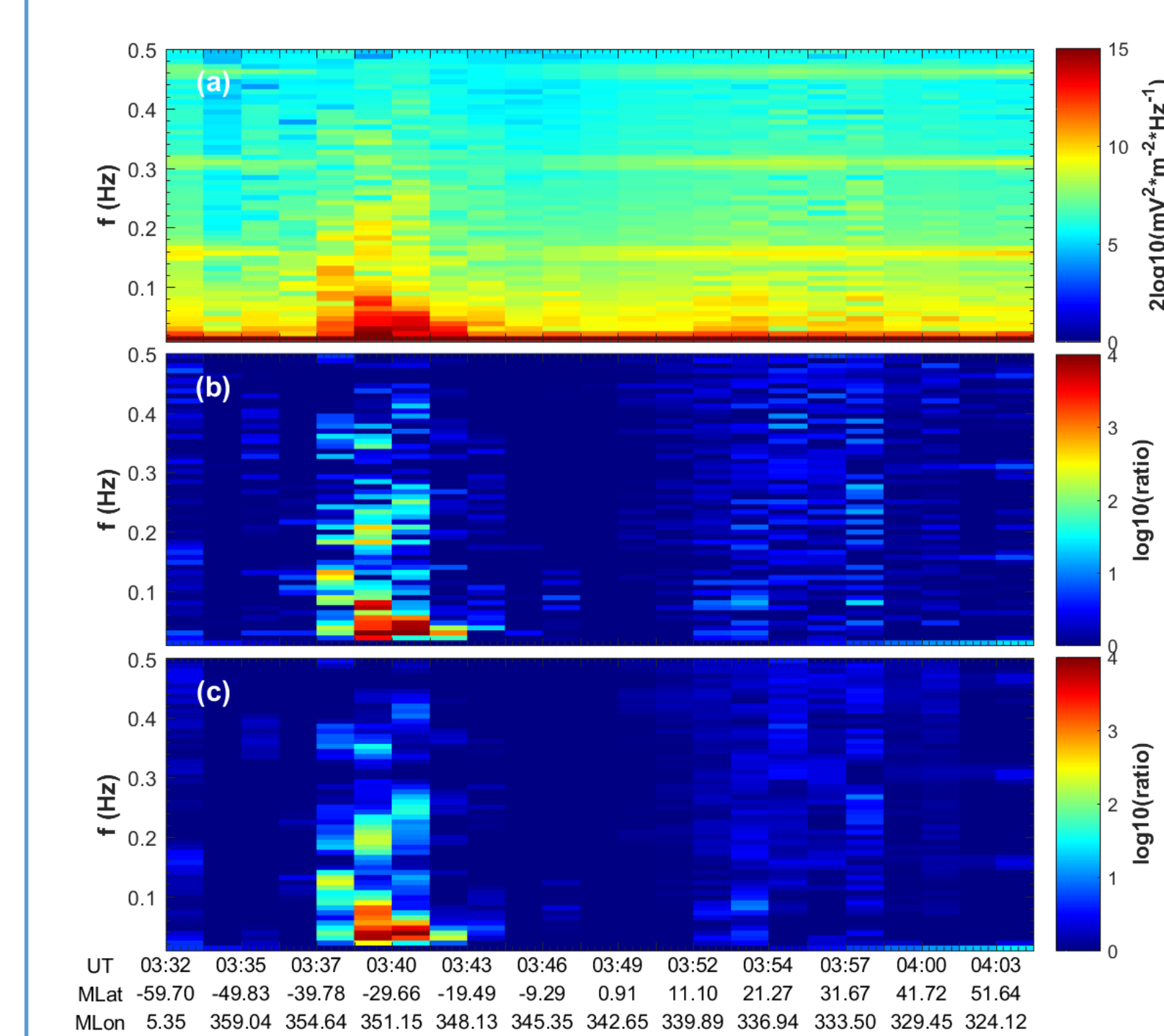


Figure 3. An example of a dynamic spectrogram of total cross-covariance power

along a half-orbit on the nightside on January 9, 2010.

- Original dynamic spectra
- Spectra with the background noise removed
- Moving averaged spectra.

Two main steps to automatically detect ULF wave events:

- Spectral peaks are identified based on the dynamic spectra along each half-orbit (e.g., Figure 3c), which exceed the background spectra by at least one order of magnitude.
- Spectral peaks in consecutive time segments are grouped into individual wave events. Spectral peaks need to satisfy the conditions of minimum duration (~ 6 mins in our case) and spectral continuity to be treated as an event.

2.4 Statistical survey of nightside ULF waves in the ionosphere

A total of 41,343 wave events related to 17,570 half-orbits are detected (referred to in the following as the **O2019 list**)

7,701 half-orbits with significant ULF oscillation identified by the selection criteria of type I and II events in Ouyang et al. (2018), labelled in the following as the **O2018 list**.

Table 1. Relationship between O2019 and O2018 lists

| Items | No. of related half-orbits | Category |
|----------------------------------------------|----------------------------|-----------------|
| O2019 list | 17,570 | Type I, II, III |
| O2018 list | 7,701 | Type I, II |
| Overlap between O2019 and O2018 lists | 6,938 | Type I, II |
| Difference (O2019 list- Overlap) | 10,632 | Type III |

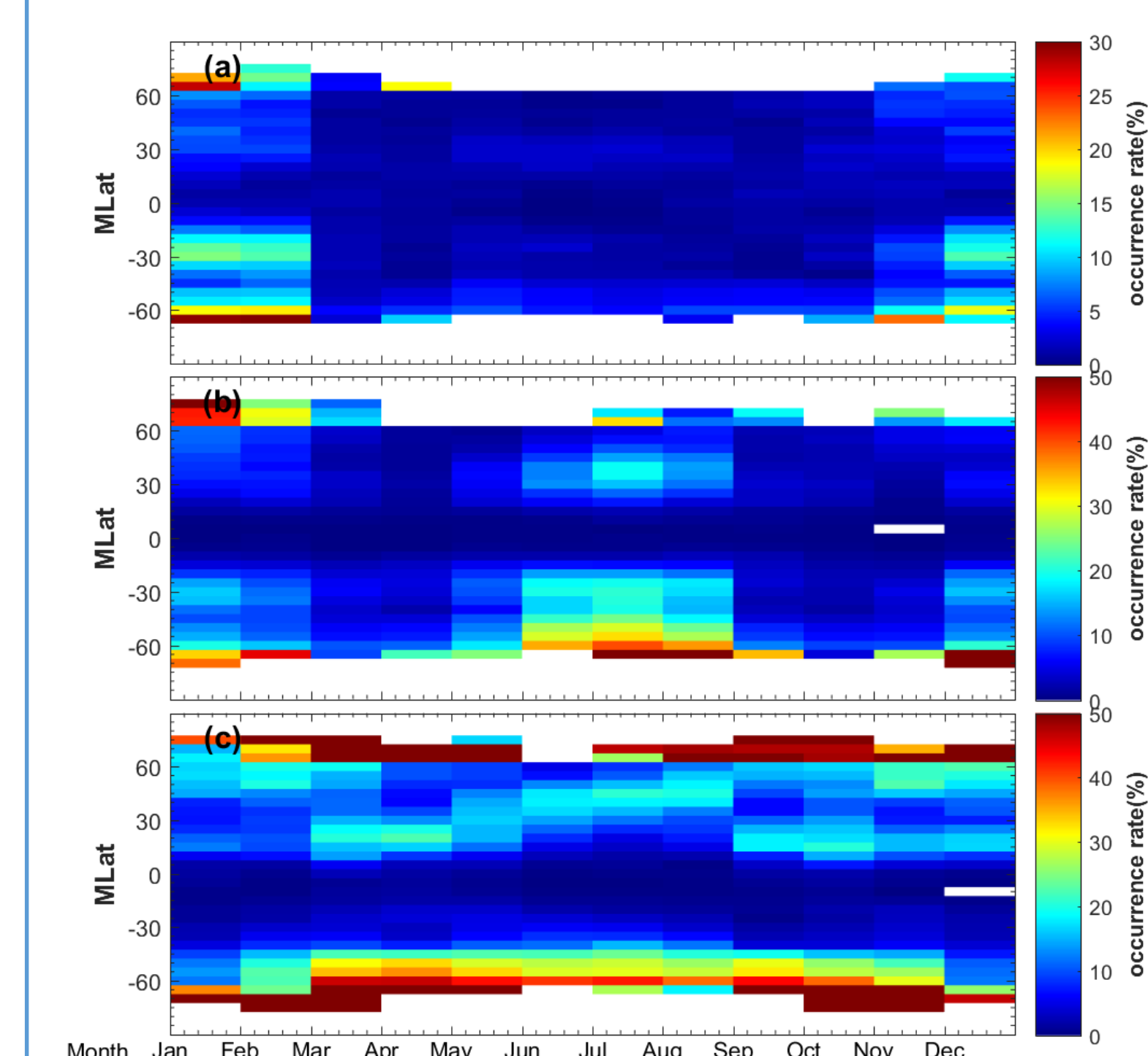


Figure 4. The occurrence rate of ULF waves versus magnetic latitude (5° bins) in every month on the nightside from May 2005 to November 2010.

- Type I & II are categorized into non-magnetospheric ULF waves
- Type III events, more likely related to magnetospheric ULF waves.

Note that results in bins at $|Mlat|>65^\circ$ are not credible due to very low data coverage.

Type I & II wave events: a clear seasonal dependence with increased occurrence rates in the local winter in the northern hemisphere (NH) and in both local winter and summer in the southern hemisphere (SH).

Type III events: the occurrence maximizes close to equinoxes (March-April and September-October), this being particularly visible at high latitudes in the SH and low latitudes in the NH.

3 Characteristics of ULF wave types during geomagnetic storms

3.1 Storm identification

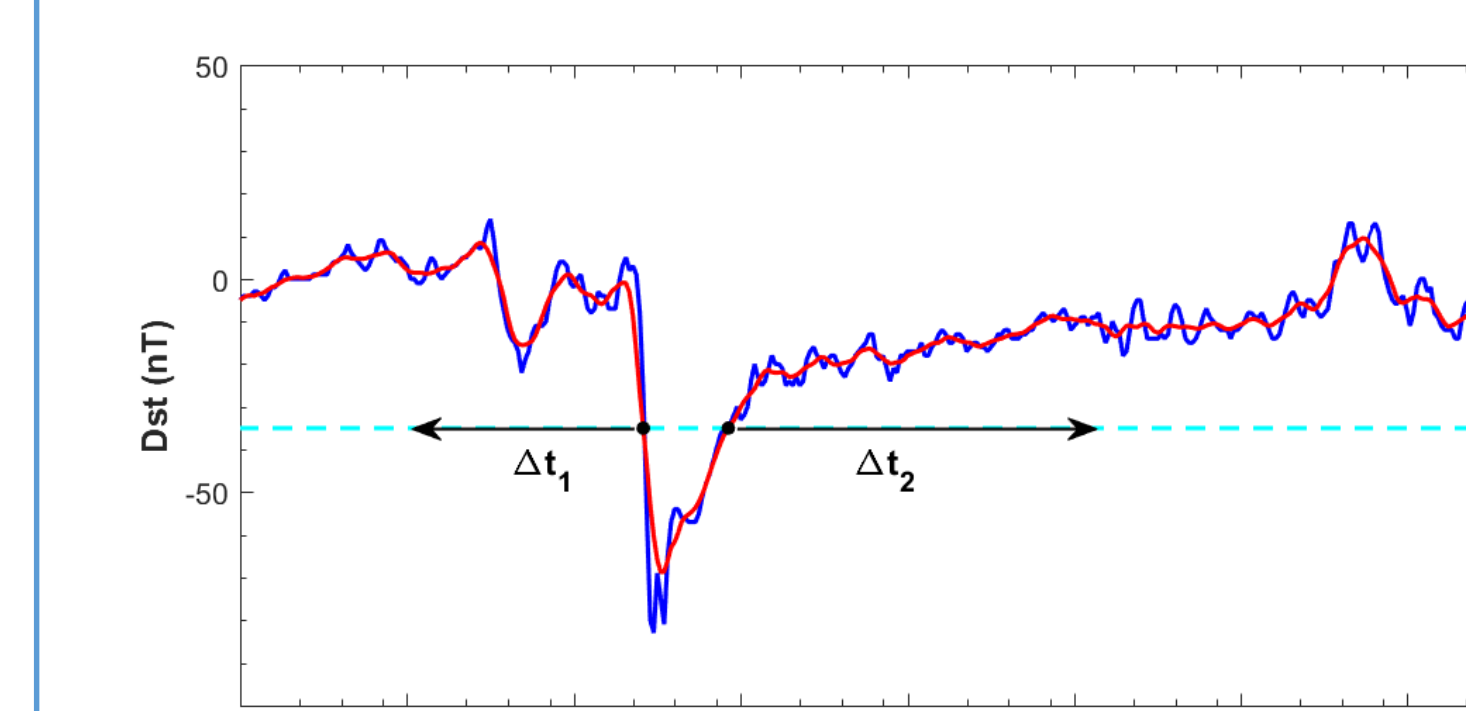


Figure 5. An example of an isolated storm.

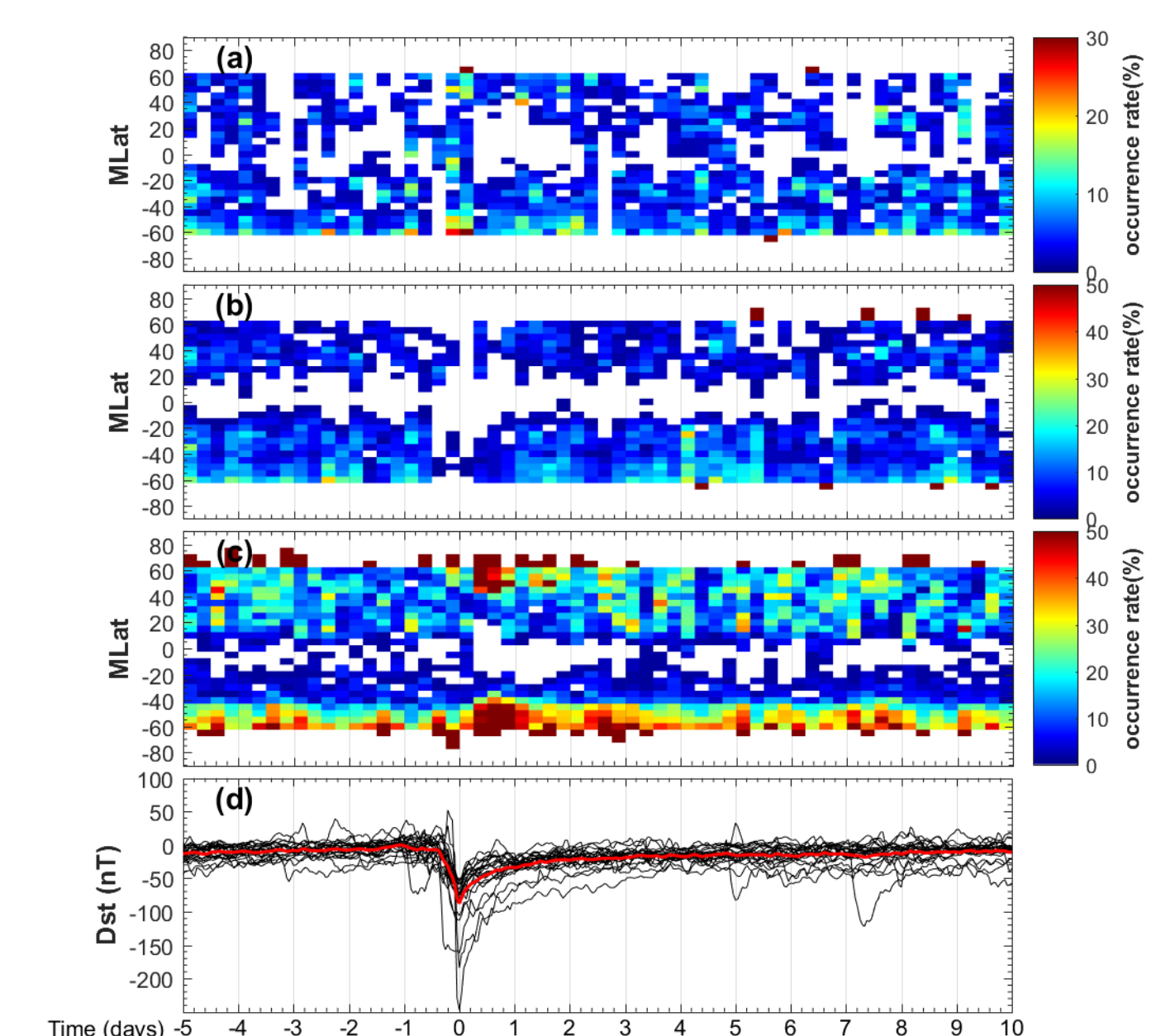
The dashed cyan line indicates the quiet threshold value (the minimum of either $0.35 * Dst_{\min}$ or -35 nT), which has two intersections (black dots) with the smoothed Dst time series (red line). Based on these two intersections, Dst value must be larger than the quiet threshold value during the entire length of Δt_1 (at least ≥ 3 days) and Δt_2 (at least ≥ 5 days).

23 isolated storms are finally selected

3.2 Superposed epoch analysis

Figure 6. Superposed epoch analysis of ULF waves relative to geomagnetic storms.

The occurrence rate of ULF waves is organized in bins of six-hour by 5° magnetic latitude for the non-magnetospheric category: (a) type I, (b) type II; as well as (c) type III wave events. (d) Dst values for 23 isolated storms (black lines) and the mean Dst value of 23 isolated storms (red line).



(a-b) Type I and type II, wave events ($L<2$, $\sim|Mlat| < 45^\circ$) do not exhibit a close correspondence with the evolution of Dst values.

(c) Occurrence rate increases significantly both in southern and northern latitudes six-hour after t_0 (the time of the Dst_{\min}), with the largest occurrence rate occurring in one day after t_0

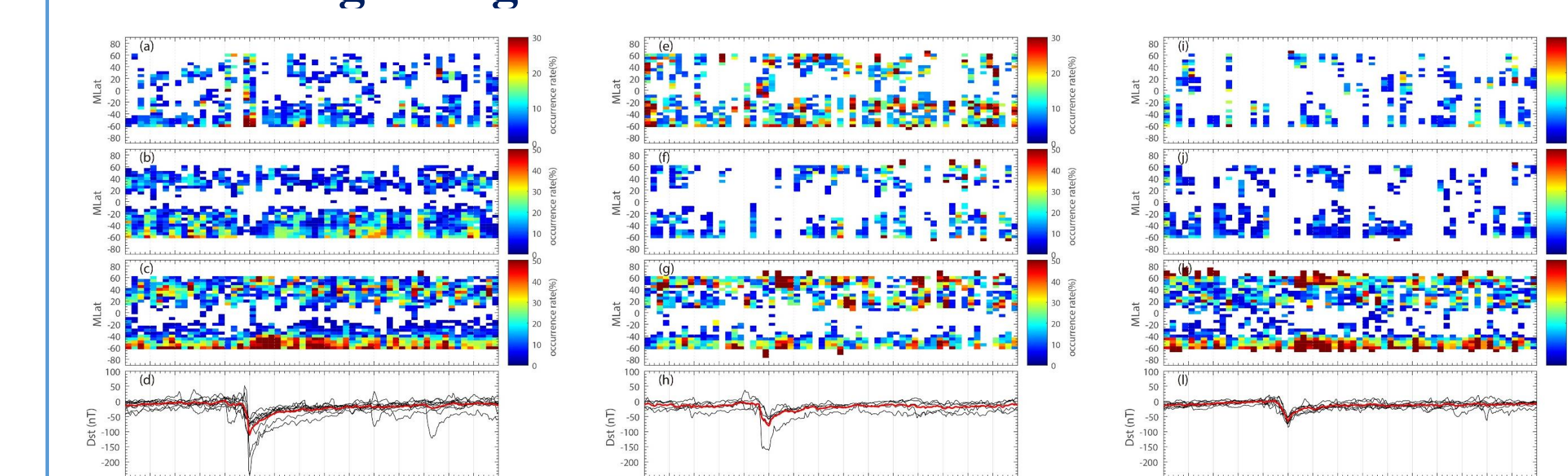
4 Discussion

Type III waves occurs almost throughout the year, with higher occurrence rate at higher latitudes, and shows a clear correlation with storms, is **most likely to be of magnetospheric origin**.

In this study, we have obtained a **global view of interhemispheric asymmetries** in ULF wave occurrence

Ionospheric conductivity is larger in the summer hemisphere, which may lead to a good reflection of ULF waves with consequently small total electric field in the ionosphere.

Storms in NH are twice as many as those in SH summer. To check whether the interhemispheric asymmetry results from the seasonal effect, see **Figure 7. Superposed epoch analysis of ULF waves relative to geomagnetic storms occurred in different seasons.**



(a)-(d) type I, type II, type III and Dst values (black lines) and the mean Dst (red line) of 10 storms in the NH summer.

(e)-(h) results for 5 storms occurred in the SH summer.

(i)-(l) results for 8 storms occurred during equinoxes.

Taking apart the seasonal effect, these results still indicate the interhemispheric asymmetry of ionospheric conductivity at nighttime with generally larger conductivities (hence denser ionosphere) in the NH

5 Conclusions

- ULF waves of non-magnetospheric and magnetospheric origins occur in the ionosphere
- Non-magnetospheric ULF waves present seasonal variations but have no clear response to storms
- Magnetospheric ULF waves show clear association with the recovery phase of storms but have no obvious seasonal variations
- An interhemispheric asymmetry with higher magnetospheric ULF wave occurrence rate in the southern hemisphere around storms indicates that the ionospheric conductivity in the southern hemisphere would be lower than in the northern hemisphere at nighttime